Microreactors for Syngas Conversion to Higher Alkanes: Characterization of Sol−Gel-Encapsulated Nanoscale Fe−Co Catalysts in the Microchannels

ARTICLE *in* INDUSTRIAL & ENGINEERING CHEMISTRY RESEARCH · JUNE 2005

Impact Factor: 2.59 · DOI: 10.1021/ie0487484

9 AUTHORS, INCLUDING:

Upali Siriwardane
Louisiana Tech University
97 PUBLICATIONS **1,028** CITATIONS
SEE PROFILE

Naidu V Seetala
Grambling State University
52 PUBLICATIONS **226** CITATIONS
SEE PROFILE

Ji Fang
Louisiana Tech University
44 PUBLICATIONS **482** CITATIONS
SEE PROFILE

Debasish Kuila
North Carolina Agricultural and Technical St…
52 PUBLICATIONS **603** CITATIONS
SEE PROFILE

Microreactors for Syngas Conversion to Higher Alkanes: Characterization of Sol−Gel-Encapsulated Nanoscale Fe−Co Catalysts in the Microchannels

Venkata S. Nagineni,[†,‡] Shihuai Zhao,[†] Avinash Potluri,[†] Yu Liang,[†] Upali Siriwardane,[‡] Naidu V. Seetala,[§] Ji Fang,[†] James Palmer,[†,∥] and Debasish Kuila*[,†,‡]

Institute for Micromanufacturing (IfM), Louisiana Tech University, Ruston, Louisiana 71272, Chemistry Program, Louisiana Tech University, Ruston, Louisiana 71272, Department of Physics, Grambling State University, Grambling, Louisiana 71245, and Chemical Engineering Program, Louisiana Tech University, Ruston, Louisiana 71272

Silicon microreactors have been coated with mixed-metal Fe−Co Fischer−Tropsch catalysts in alumina sol−gel for conversion of syngas ($CO + H_2$) to higher alkanes. Characterization of the nanocatalysts using scanning electron microscopy, energy-dispersive X-ray, atomic force microscopy, and Brunauer−Emmett−Teller surface area measurements, packaging, and the reaction results from a mass spectrometer at controlled temperatures (200−260 °C) and pressure (1 atm) with varying H_2:CO ratios from 1:1 to 10:1 are described. The catalyst does not adequately infiltrate the 5-μm channels; it coats nicely the 25-μm channels. The initial results are consistent with a lower conversion of CO (∼32%) in a 5-μm-channel reactor and a higher conversion (∼52%) in a 25-μm-channel reactor. The selectivity to propane (∼80%) is not affected by the width of the microchannels. The activity of the sol−gel-encapsulated catalyst before and after the reactions is estimated from its magnetic properties using a vibrating sample magnetometer.

Introduction

A major concern in countries with high reserves of natural gas is the lack of infrastructure and technology to ship these valuable reserves to larger economies. Gas-to-liquid (GTL) technology converts gases to liquids that are easier to transport. It has become a major revolution in the petroleum industry with a low cost of production and access to a much bigger diesel fuel market.[1] Fischer−Tropsch (F−T) synthesis makes use of GTL technology in converting the unconsumed natural gases into hydrocarbons, which are subsequently converted to fuels by hydrocracking.[2,3] At present, several corporations such as Exxon-Mobil, Shell, Sasol, Syntroleum, and Rentech are involved in liquefying natural gas.[4,5] Thus, catalyst development for GTL technology using F−T synthesis is an active area of research.

The catalysts for F−T synthesis generally contain metals such as cobalt, iron, nickel, and copper with support materials such as oxides and zeolites. More specifically, the influence of various support materials such as titania,[6,7] alumina,[7−9] silica,[10] and ceria[11] on the activity of cobalt catalysts for CO conversion has been studied. Alumina is often used as a support for cobalt catalysts because of its thermal stability, though reduction of cobalt oxide to cobalt is limited as a result of the strong interaction between the support and cobalt oxides.[12,13] The addition of a second catalyst like iron may improve the selectivity to heavier alkanes with less selectivity to methane.[14] Recent studies indicate that the catalyst activity depends on the number of active sites located on the surface of the support formed by the reduction process, determined by the particle size, loading, and the degree to which the metal has been reduced.[15−17]

The development of the catalyst and its support is a major thrust of our research and others[18] for conversion of syngas to higher alkanes. Microreactors are ideal systems for catalyst development because they not only provide unique advantages such as low consumption of reactants and greater speeds in catalyst characterization but also are suitable for easy integration with other devices.[19,20] They require less space, materials, and energy, have shorter response times, and provide inherent safety of operation.[21] More significantly, the high surface area of microchannels to the volume of the reactor inhibits gas-phase free-radical reactions and improve heat transfer for exothermic reactions.[22,23] Here, we report the fabrication of a micron-size multichannel Si reactor, deposition and characterization of sol−gel-encapsulated iron and cobalt catalysts in the microchannels, microreaction setup, and initial catalysis results on exothermic syngas conversion to higher alkanes.

Materials and Methods

The silicon wafers were purchased from Montco Silicon Technologies, Inc. (Spring City, PA). The microreactors with the desired microchannel dimensions were fabricated using photolithography and an inductively coupled plasma (ICP) etching procedure at the Institute for Micromanufacturing (IfM), Louisiana Tech

* To whom correspondence should be addressed. E-mail: dkuila@latech.edu.
[†] IfM, Louisiana Tech University.
[‡] Chemistry Program, Louisiana Tech University.
[§] Grambling State University.
[∥] Chemical Engineering Program, Louisiana Tech University.

10.1021/ie0487484 CCC: $30.25
Published on Web 06/23/2005

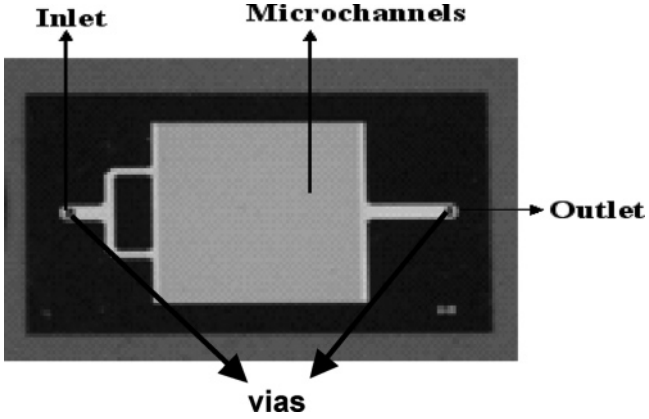

Figure 1. Typical silicon microreactor (3.1 × 1.6 cm), used for F−T synthesis, containing 5-μm-wide and 100-μm-deep microchannels.

University. Aluminum tri-*sec*-butoxide (Aldrich Chemicals, Milwaukee, WI) and ferric nitrate and cobalt nitrate (Sigma-Aldrich, St. Louis, MO) were used for preparation of the sol−gel-encapsulated catalyst. Gases of ultrahigh-purity hydrogen (Aeriform Corp., Houston, TX) and carbon monoxide (purity 99%, Aldrich Chemicals, Milwaukee, WI) were used as feeds for syngas. Ultrahigh-purity helium (Aeriform Corp., Houston, TX) was used to dilute the gas exiting the reactor prior to its analysis in a Stanford Research System 200 mass spectrometer.

Experimental Section

Microreactor Design and Fabrication. The reactor is a microchannel device (Figure 1), 3.1 cm × 1.6 cm, with a reaction area of 1.3 cm × 1.2 cm, and consists of feed inlet, product outlet, and microchannels of 5 or 25 μm width and 100 μm depth. The microreactor is made from a 4-in.-diameter, 500-μm-thick, double-side-polished silicon ⟨100⟩ wafer, fabricated using standard photolithography and deep dry etching (ICP etching),[24,25] and it is very much like that used in the integrated-circuit industry.

The implementation of fabrication involves three chrome photomasks for pattern transfer: microchannel area, inlet and outlet distributors, and the fluidic vias (Figure 1). The pattern (with eight reactors on each mask) was transferred onto a ⟨100⟩ 500-μm-thick Si wafer by photolithography. A front-side alignment and a back-side alignment with tolerances of 1−2 μm were performed with a EVG 420 aligner machine. Positive photoresists, Microchem 1813 for the front side and AZ 9260 for the back side, were used for pattern transfer from the masks to the silicon wafer. Hexamethyldisiloxane is the promoter for better adhesion between the photoresist and silicon. The front-side alignment ensures that the channels are connected with the inlets and outlets, and the back-side alignment allows the fluidic vias to interface the microreactor with the inlets and outlets. The ICP etching is then used to generate front-side via, inlet, microchannel outlet patterns, and back-side via for reactant flow into the microchannels. The designed microreactors have been tested for prototype reactions described elsewhere.[26−28]

Catalyst Preparation, Deposition in the Microchannels, and Activation. Alumina sol−gel was deposited in the microchannels of the reactor as a catalyst support. The basic steps involve the hydrolysis of aluminum alkoxide to form its hydroxides and polycondensation of aluminum hydroxide to alumina.[29] The parameters that affect the sol preparation are the relative amounts of acid or base, water, and alkoxide and temperature.[30,31] The alumina precursor, aluminum tri-*sec*-butoxide, was added dropwise into water at 80 °C, followed by the addition of nitric acid to reach the molar ratio of 1:100:4 (aluminum tri-*sec*-butoxide−water−nitric acid). The solution was stirred vigorously for ∼30 min until a clear mixture was obtained. The reaction solution was refluxed overnight for ∼12−14 h at 90 °C and cooled to 60 °C. The solutions of ferric and cobalt nitrate salts prepared in water were then added in the desired composition (12% loading of each) to the alumina sol until a complete dispersion was obtained. The sol-containing catalysts (in nitrate forms) were used for coating of the microchannels of the reactor followed by drying with gentle heating. During the process of aging, polycondensation leads to cross-linking and the formation of polymers of alumina. The sol−gel-coated reactor was then treated with a 10% NH_4OH solution for about 30 min to form hydroxides, followed by washing with water and drying in a vacuum oven for 30 min at 60 °C. The oxides of cobalt and iron were finally reduced to active metals in a continuous flow of hydrogen at 450 °C for 4 h after calcination.

Packaging of the Reactor. To protect the device from the environment and to avoid leakage of the reactants, anodic bonding was used for packaging of the microreactor device. This procedure is simple and has attracted great interest because it provides a strong bonded-hermetic seal. Pyrex glass, used for packaging of the reactor, had the same dimensions as the reactor. The surface of the reactor and the glass were first cleaned properly with acetone and water in order to remove any particulate matter that would otherwise interfere with the bonding process. The microreactor was placed in the furnace at 500 °C, with the Pyrex glass connected to a cathode and the silicon−reactor connected to an anode. A voltage of 700 V was applied for 45 min to yield a high bonding strength between the glass and the reactor.[32]

The packed reactor was reactivated in the presence of hydrogen at 300 °C for few hours, before the catalytic reaction studies, to eliminate any deactivation of the catalyst due to exposure to the atmosphere during packaging.

Characterization of the Catalyst and Its Support. The surface area measurement of sol−gel-encapsulated catalysts was performed on flat silicon chips using the Brunauer−Emmett−Teller (BET) method with nitrogen as an adsorbate. Measurements were performed in a Quantachrome NOVA 2000 for the alumina sol−gel-encapsulated catalysts that yield surface areas for a gram of the sol−gel-containing catalyst. While atomic force microscopy (AFM) images were recorded using a Quesant Q-scope 250, Carl Zeiss DSM 942 scanning electron microscopy (SEM) along with an energy-dispersive X-ray (EDX) system was used to study the uniformity and elemental composition of sol−gel-encapsulated catalysts deposited in microchannel reactors. The EDX spectrometer is equipped with a Super Quantum Dry Si (Li) detector that has an elemental analysis capability in the wide range from boron to uranium with better than 145-eV resolution. The magnetization properties of Al_2O_3 sol−gel-encapsulated Co−Fe nanocatalysts in the microreactors were

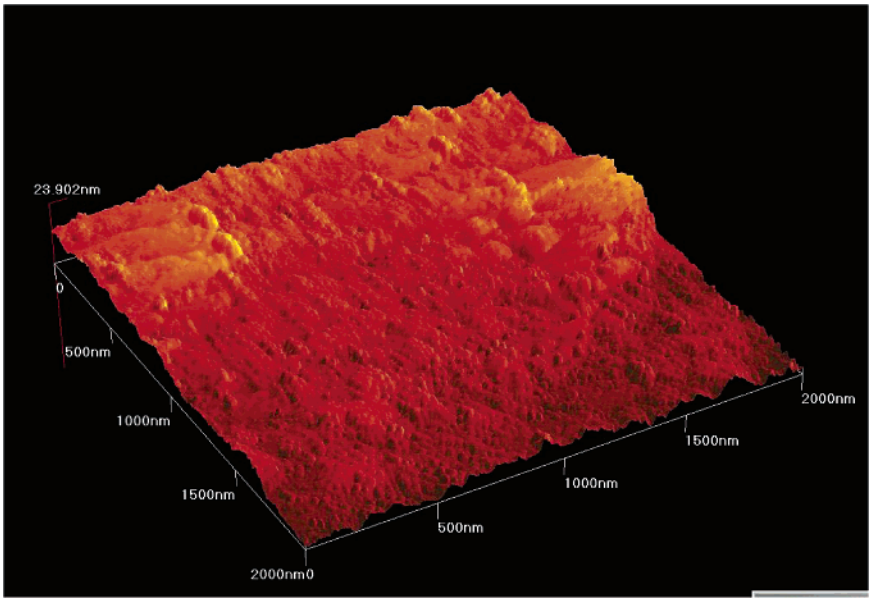

Figure 2. AFM image of alumina sol−gel-encapsulated Fe−Co catalysts (picture taken on a glass slide).

Table 1. Elemental Composition from EDX Analysis for Alumina Sol−Gel-Encapsulated Catalyst(s) Using Metal Nitrate Solutions and Metal Oxide Nanoparticles

alumina sol−gel-encapsulated iron and cobalt	intended metal composition		EDX results	
	% Fe loading	% Co loading	% Fe loading	% Co loading
metal nitrate solutions	12	12	2.5	3.7
metal oxide nanoparticles	12	12	8.1	9.4

determined using a Digital Measurement Systems 880A vibrating sample magnetometer (VSM) before and after the syngas reactions.

Experimental Setup for Microreaction Studies. The experimental setup consists of a reactor block, flowmeters, pressure gauges, and a mass spectrometer. LabVIEW software is used to control the flow of the feed gas and to maintain the temperature within the reactor. The reaction products from the outlet of the reactor are diluted with He before the mixture is fed to a mass spectrometer (residual gas analyzer, RGA). The software of the RGA records the partial pressures of the outlet gases that were detected in the mass spectrometer. First, a reference base is made by flowing CO and H_2 through the reactor without any catalyst. Then, the partial pressures of the reactant and product gases are used to calculate the conversion of CO and the selectivity to higher alkanes.

Results and Discussion

Characterization of Sol−Gel-Encapsulated Catalysts. Heterogeneous catalytic reactions occur at the fluid−solid interface, and a large surface area is essential to attain a significant reaction rate. To improve the surface area, we have considered deposition and activation of the alumina sol−gel-encapsulated Fe−Co catalyst in the microchannels. The surface area measurements by the BET method for alumina-supported catalysts yield an average specific surface area of 285 m^2/g. This is due to the high porosity of alumina generated by sol−gel processing. An AFM image of the porous alumina sol−gel-deposited on a glass plate is shown in Figure 2. The diameter of the alumina granules formed by the sol−gel procedure is in the range of 40−150 nm. It is expected that the diameter of the iron and cobalt catalysts would be less than 100 nm when they are encapsulated in the alumina sol−gel matrix.

To optimize the sol−gel preparation and catalyst deposition in the microchannels, the composition of sol−gel containing nanoscale Fe and Co has been studied. The results of the EDX analysis are shown in Table 1. The intended metal composition of Fe−Co based on the solution mixture using metal nitrates was 24% (12% each). However, the EDX analysis shows only 5−7% of Fe−Co catalyst in the hydrogenated reactor. To have a better understanding of the nanocatalyst, we have separately synthesized CoO nanoparticles (15−30 nm) and used commercially available Fe_2O_3 nanoparticles (10−40 nm) as catalyst precursors in the sol−gel matrix.[33,34] The EDX analysis of these systems is included in Table 1. The data suggest that the metal oxide nanoparticle method yields much higher metal loading compared to that obtained by the metal nitrate procedure. However, because the synthesized and commercial nanoparticles are not uniformly dispersed in a sol−gel matrix and in order to develop a simplified procedure to deposit nanocatalysts directly in the microchannels, we have considered the metal nitrate procedure for our present studies.

SEM imaging of the microchannels, coated with a sol−gel-encapsulated catalyst, was performed to monitor the deposition of the sol−gel in the microchannels. Figure 3 shows that only a small amount of alumina has infiltrated the 5-μm microchannel, retaining the majority of the sol−gel on the top of the channels. Although our AFM studies show that the sol−gel granules are ~100 nm in diameter, the highly viscous nature likely prevents the sol−gel from passing through the 5-μm channels. Indeed, this is supported by the SEM image of the sol−gel in the 25-μm channels, where the catalyst is dispersed throughout the channels (Figure 4).

Conversion and Selectivity. Although the observed loading of sol−gel-encapsulated Fe−Co catalysts in the microchannels is low, they show significant activity toward the synthesis of alkanes. The alumina-encapsulated mixed iron and cobalt produce methane, ethane,

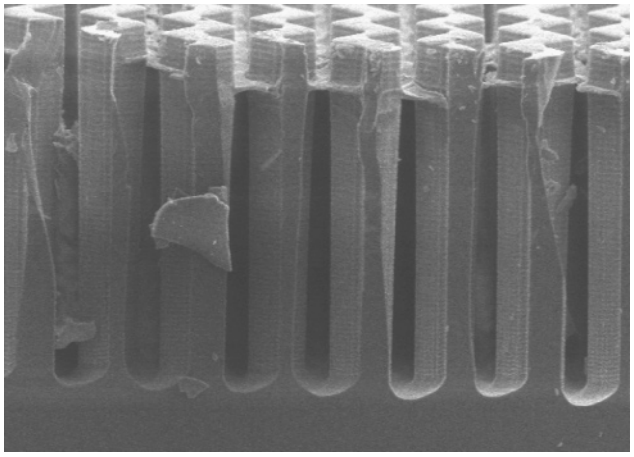

Figure 3. SEM image of an alumina sol−gel-encapsulated Fe−Co catalyst deposited on a 5-μm-wide-channel microreactor showing incomplete deposition in the 100-μm-deep channels.

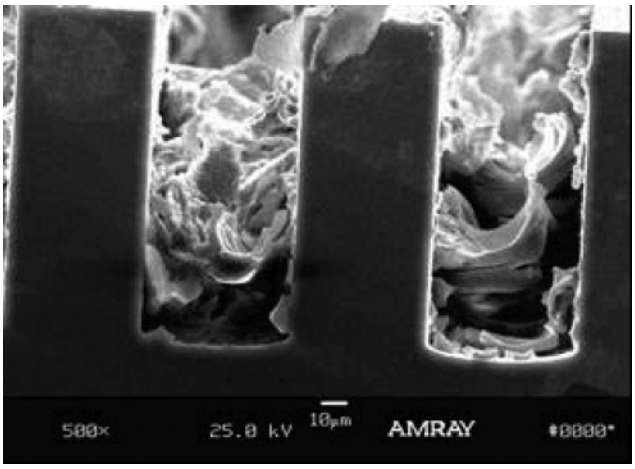

Figure 4. SEM image of an alumina sol−gel-encapsulated Fe−Co catalyst deposited on a 25-μm-wide-channel microreactor showing complete deposition in the 100-μm-deep channels.

and propane, as presented in the equation and discussion below.

$$CO + H_2 \xrightarrow[\text{Fe−Co on } Al_2O_3 \text{ support}]{200-300\ ^\circ C} CH_4 + C_2H_6 + C_3H_8 + \text{higher alkanes}$$

(a) Conversion of CO. Initial studies were performed in 5-μm-channel reactors to study the conversion rates at different ratios of H_2−CO. Figure 5 shows conversion of CO with respect to the ratio of H_2−CO at a total flow rate of 0.6 sccm and 230 °C in 5-μm-channel reactors. The conversion is maximum (~32%) when the H_2−CO ratio is ~3 and then gradually decreases with a further increase in the ratio of H_2−CO.

We wondered about low F−T conversion in 5-μm-channel reactors (Figures 5 and 6). We surmised that a lower CO conversion (~32%) is most likely due to insufficient coating of the sol−gel in the microchannels of the reactor as discussed above. This is indeed supported by higher conversion in 25-μm-channel reactors (top curve of Figure 6) where the sol−gel can penetrate easily (shown above in Figure 4), allowing the reactants to have more interaction with the catalyst. However, the volume of the microreactor is ~9 mm^3 for both 5-μm (1200 in number) and 25-μm (240 in number) wide channel reactors.

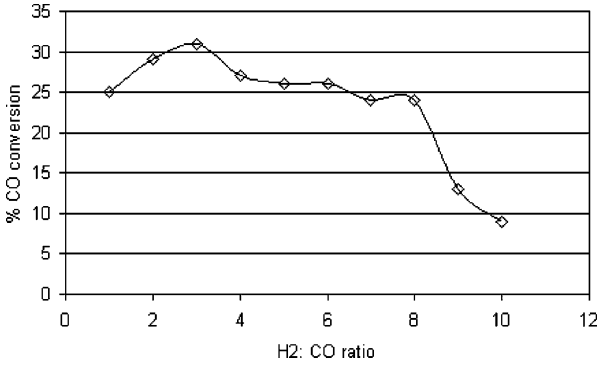

Figure 5. Conversion of CO to alkanes in a 5-μm-channel reactor with different H_2−CO ratios at 230 °C and 1 atm.

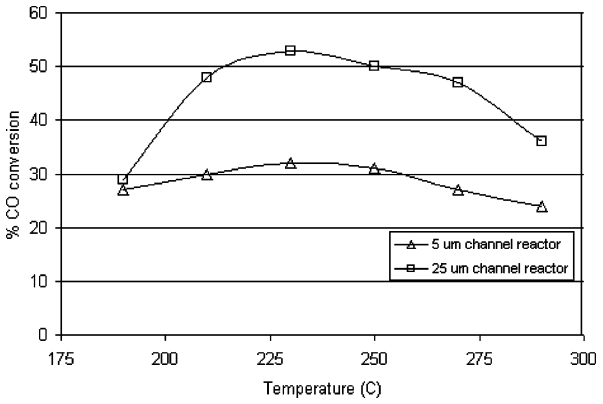

Figure 6. Comparative studies on the conversion of CO to alkanes in 5- and 25-μm-channel reactors at different temperatures, a fixed H_2−CO ratio of 3:1, and 1 atm.

We have also optimized the reaction conditions by studying the reactions at different temperatures (Figure 6). The conversion of CO initially rises with an increase in the temperature. The highest conversion of CO is achieved ~52% (~32% in the 5-μm reactor) at 230 °C with a H_2−CO ratio of 3:1 in 25-μm-channel reactors. After that, the conversion of CO decreases with an increase in the temperature due to the exothermicity of the reaction as the competition between activation and exothermicity progresses. This is consistent with that observed with the reaction in the macroscale.[35] The blockages of catalyst active sites may occur as a result of carbon formation from the water gas shift reaction and can also decrease conversion at higher temperature. The effect of the flow rate of syngas was also investigated. The reaction results show that the conversion of CO decreases with an increase in the total flow rate as a result of a decrease in the residence time of the reaction.

(b) Selectivity to Different Alkanes. Although the conversion of CO is affected by the width of the channels, the selectivity toward different alkanes is not. The selectivity of CO to each product was defined as the percentage of each product by the calculation of the partial pressure of each product divided by the total partial pressure of all products from the mass spectrometer. Figure 7 shows the selectivity to methane, ethane, and propane as a function of the temperature in 5- and 25-μm channel reactors. Propane has been the major product of the reaction in both cases, with a selectivity up to 78%. In contrast to CO conversion, the residence time does not have any significant effect on the selectivity to alkanes in the microreactor.

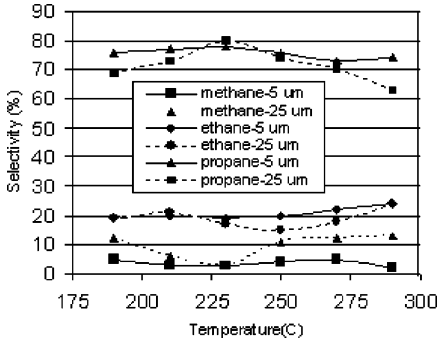

Figure 7. Selectivity of alkanes—methane, ethane, and propane—in 5- and 25-μm-wide-channel reactors at 230 °C, a H_2—CO ratio of 3:1, and 1 atm.

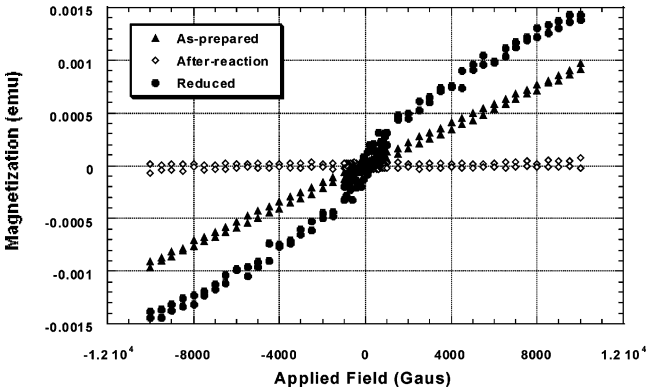

Figure 8. VSM studies of alumina sol—gel-encapsulated Fe—Co catalysts: after preparation (paramagnetic), after reduction with hydrogen (ferromagnetic), and after the F—T reaction in a microreactor.

Magnetization Studies. One of the advantages of Fe and Co is their ferromagnetic behavior besides catalytic properties. Previous studies have shown significant changes in the saturation magnetization (M_s) for a number of ferromagnetic catalysts as a result of chemisorptions of H_2 and CO.[36,37] To understand the nature and activity of the catalyst at different stages of the reactions, magnetization studies were performed using a VSM. Figure 8 shows magnetic properties of alumina sol—gel (-encapsulated Co and Fe catalysts) coated microreactors after calcination and reduction with hydrogen and at the end of the syngas ($CO + H_2$) reaction. The deposited catalyst in the reactor shows paramagnetism due to iron and cobalt oxides. Because iron and cobalt oxides are reduced to pure metals during hydrogenation, ferromagnetic behavior is observed.[36,37]

The ferromagnetic component of the catalyst mixture can be estimated using saturation magnetization of the samples. A lower limit of ~40% for the reduction efficiency due to hydrogenation at 450 °C for 4 h is obtained. The ferromagnetic behavior almost disappears in the post catalytic reaction sample. Presumably, the active Fe and Co metals form inactive compounds such as cobalt carbonyls and iron carbides[37—39] during the catalytic reactions, and thus the ferromagnetic nature decreases. The magnetic data indicate that ~85% of the catalyst is inactive after 25 h of the reaction. More systematic studies are currently underway to have a better understanding of the magnetochemical characteristics of these catalysts.

Conclusions

We have done initial studies of syngas conversion using a mixed iron and cobalt catalyst encapsulated in the alumina sol—gel in 5- and 25-μm-wide-channel Si microreactors. The surface area measurements reveal that the sol—gel support improves the surface area significantly, allowing more interaction between the catalysts and reactants. The EDX analysis shows much lower metal (Fe—Co) loading in the alumina sol—gel than the intended composition from metal nitrate solutions. The metal loading is improved by incorporating metal oxide nanoparticles (Fe_2O_3—CoO) in the sol—gel. The 25-μm-channel reactors are found to be more effective in the syngas conversion with a maximum yield of ~52% compared to the 5-μm channels, where the maximum conversion of CO is ~32%. The syngas conversion is also influenced by the H_2—CO ratio of the feed gas and temperature. The highest conversion of CO is achieved at a H_2—CO ratio of ~3:1 at 230 °C. Magnetization studies indicate that the hydrogenation of cobalt and iron oxides to a reduced metal has an efficiency of ~40%. The ferromagnetic behavior shows that 85% of the catalyst is inactive after 25 h of the catalytic reactions.

Acknowledgment

We gratefully acknowledge the financial support of NSF-EPSCoR. We thank Dr. K. Varaharamyan, S. Vegesna, and R. K. Aithal for their suggestions and help in this project.

Literature Cited

(1) Tullo, A. H. *Chem. Eng. News* **2003**, *81*, 18.
(2) Das, T. K.; Jacobs, G.; Patterson, P. M.; Conner, W. A.; Li, J.; Davis, B. H. *Fuel* **2003**, *82*, 805.
(3) Choudhry, V. R.; Sansare, S. D.; Rajput, A. M. *Indian* **1997**, IN 1784470, 23.
(4) Steynberg, A. P.; Espinoza, R. L.; Jager, B.; Vosloo, A. C. *Appl. Catal. A* **1999**, *186* (1—2), 41.
(5) Espinoza, R. L.; Steynberg, A. P.; Jager, B.; Vosloo, A. C. *Appl. Catal. A* **1999**, *186* (1—2), 13.
(6) Iglesia, E. *Appl. Catal. A* **1997**, *161* (1—2), 59.
(7) Iglesia, E.; Soled, S. L.; Fiato, R. A.; Via, G. H. *J. Catal.* **1993**, *143*, 345.
(8) Kogelbauer, A.; Goodwin, J. G.; Oukaci, R. J. *J. Catal.* **1996**, *160*, 125.
(9) Schanke, D.; Hilmen, A. M.; Bergene, E.; Kinnari, K.; Rytter, E.; Adnanes, E.; Holmen, A. *Energy Fuels* **1996**, *10*, 867.
(10) Sun, S.; Tsubaki, N.; Fujimoto, K. *Appl. Catal. A* **2000**, *202*, 121.
(11) Niemela, M. K.; Krause, A. O. I.; Vaara, T.; Kiviaho, J.; Reinikainen, M. *Appl. Catal. A* **1996**, *147*, 325.
(12) Vada, S.; Hoff, A.; Adnanes, E.; Schanke, D.; Holmen, A. *Top. Catal*. **1995**, *2*, 155.
(13) Schanke, D.; Veda, S.; Blekkan, E. A.; Hilman, A. M.; Hoff, A.; Holmen, A. *J. Catal.* **1995**, *156*, 85.
(14) Li, S.; Krishnamoorthy, S.; Li, A.; Meitzer, G. D.; Iglesia, E. *J. Catal.* **2002**, *206*, 202.
(15) Sun, S.; Fujimoto, K.; Yoneyama, Y.; Tsubaki, N. *Fuel* **2002**, *81*, 1583.
(16) Iglesia, E.; Soled, S. L.; Fiato, R. A.; Via, G. H. *J. Catal.* **1993**, *143* (2), 345.
(17) Matsuzaki, T.; Takeuchi, K.; Hanaoka, T.; Arakawa, H.; Sugi, Y. *Catal. Today* **1996**, *28* (3), 251.
(18) Benjamin, E.; Rocco, A. F.; Thomas, G. K.; Richard, F. B. *CHEMTECH* **1999**, 32.
(19) Surangalikar, H.; Besser, R. S. In *Proceedings of the 6th International Conference on Microreaction Technology (IMRET V1)*, New Orleans, LA, 2002; Renard, I., Ed.; AIChE: New York, 2002.
(20) Srinivasan, R.; et al. *AIChE J.* **1997**, *43* (11), 3059.

(21) Ehrfeld, W.; Hessel, V.; Lowe, H. *Microreactors: New Technology for Modern Chemistry*; Wiley−VCH: Weinheim, Germany, 2000; ISBN3-527-29590-9.

(22) Ouyang, S.; Prevot, M.; Surangalikar, H.; Yang, W.; Besser, R. S. *Abstracts of the Materials Research Society Fall Meeting*; Materials Research Society: Warrendale, PA, 2001.

(23) Autze, S. V.; Wille, G. *Chimia* **2002**, *56*, 636.

(24) Madou, M. *Fundamentals of Microfabrication: The Science of Miniaturization*, 2nd ed.; CRC Press: Boca Raton, FL, 1997; ISBN 0-8493-9451-1.

(25) Hill, R. *J. Vac. Sci. Technol. B* **1996**, *14*, 547.

(26) Zhao, S.; Besser, R. S. Proceedings of the AIChE Meeting, New Orleans, LA, 2002.

(27) Zhao, S. Ph.D. Dissertation, IfM, Louisiana Tech University, Ruston, LA, 2003.

(28) Zhao, S.; Nagineni, V. S.; Liang, Y.; Hu, J.; Aithal, K. R.; Naidu, S. V.; Fang, F.; Siriwardane, U.; Besser, R.; Varahramyan, K.; Palmer, J.; Nassar, R.; Kuila, D. *Microreactor*: *ACS Book Chapter* **2005**, in press.

(29) Haas-Santo, K.; Fichtner, M.; Schubert, K. *Appl. Catal. A* **2001**, 220 (1−2), 79.

(30) Brinker, C. J.; Scherer, G. W. *Sol−Gel Science: The Physics and Chemistry of Sol−Gel Processing*; Academic Press: New York, 1990.

(31) Sanchez, C.; Livage, J.; Henry, M.; Babonnean, F. *J. Non-Cryst. Solids* **1988**, *100*, 65.

(32) (a) Hanneborg, A.; Nese, M.; Ohickers, P. *J. Micromech. Microeng.* **1991**, *1*, 139. (b) Kovacs, G. T. A. *Micromachined Transducers Sourcebook*; WCB/McGraw-Hill Press: New York, 1998; ISBN 0-07-290722-3.

(33) Nagineni, V. S. M.S. Dissertation, IfM, Louisiana Tech University, Ruston, LA, 2004, and references cited therein.

(34) Kuila, D.; Nagineni, V. S.; Zhao, S.; Indukuri, H.; Liang, Y.; Potluri, A.; Siriwardane, U.; Seetala, N.; Fang, J. *Mater. Res. Soc. Symp. Proc.* **2004**, *820*, O3.4.1.

(35) Huang, X.; Roberts, C. B. *Fuel Process. Technol.* **2003**, *83*, 81.

(36) Selwood, P. W. *Chemisorption and Magnetization*; Academic Press: New York, 1975.

(37) Akundi, M. A.; Zhang, J.; Gibbs, M.; Watson, M. M.; Murty, A. N.; Naidu, S. V.; Bruster, E.; Turner, L.; Waller, F. J. *IEEE Trans. Magn.* **2001**, *37*, 2929.

(38) Belhekar, A. A.; Ayyappan, S.; Ramaswamy, A. V. *J. Chem. Technol. Biotechnol.* **1994**, *59*, 395.

(39) Sun-Kou, M. R.; Mendioroz, A.; Fierro, J. L. G.; Palacios, J. M. *J. Mater. Sci.* **1995**, *30*, 496.

Received for review December 24, 2004
Revised manuscript received April 18, 2005
Accepted May 12, 2005

IE0487484